AIP Applied Physics Letters

Experimental study of the minimum metal gate thickness required to fix the effective work function in metal-oxide-semiconductor capacitors

F. Fillot, S. Maîtrejean, I. Matko, and B. Chenevier

Citation: Applied Physics Letters **92**, 023503 (2008); doi: 10.1063/1.2833697
View online: http://dx.doi.org/10.1063/1.2833697
View Table of Contents: http://scitation.aip.org/content/aip/journal/apl/92/2?ver=pdfcov
Published by the AIP Publishing

Experimental study of the minimum metal gate thickness required to fix the effective work function in metal-oxide-semiconductor capacitors

F. Fillot,[1,a)] S. Maîtrejean,[1] I. Matko,[2] and B. Chenevier[2]
[1]*CEA-LETI, MINATEC, 17 rue des Martyrs, 38054 Grenoble CEDEX 9, France*
[2]*LMGP-UMR 5628, INPG, MINATEC, 3 parvis Louis Néel, BP 257, 38016 Grenoble, France*

(Received 25 September 2007; accepted 11 December 2007; published online 14 January 2008)

We have investigated the dependence of the effective work function (EWF) of a poly-*p*+/TiN/SiO_2/Si capacitor as a function of the TiN layer thickness. By using a pulsing chemical vapor deposition process, the nitride layer was demonstrated to be continuous from 2.2 nm. It was also shown that the EWF of capacitors, made with TiN layer thickness ranging between 2.2 and 7.1 nm, is independent of the thickness and similar to that of bulk TiN. Our study indicates that the EWF of the entire gate electrode stack is determined by the first metallic monolayers (<2.2 nm) in contact with the gate dielectric. © *2008 American Institute of Physics*.
[DOI: 10.1063/1.2833697]

Scaling of sub-45-nm complementary metal-oxide-semiconductor (CMOS) devices requires metal gate electrodes to address restricting factors of usual polysilicon gates, such as polydepletion, doping species penetration, and Fermi level pinning.[1,2] In CMOS processing, thin metallic layers could be stacked with a polysilicon layer as a cap material to form the gate electrode. The thicknesses of the layers in the stack may play a major role because it impacts the stress repartition in the structure and must be also optimized to control the gate etch. In MOS structures, the flatband voltage (V_{FB}) depends linearly to the effective work function (EWF). However, it is not known how many nanometers influence the V_{FB} and thus the EWF. Thus, it presents a physical interest to know experimentally the minimal thickness necessary to fix the gate EWF in MOS devices. It was shown with *ab initio* calculations by Park *et al.* that the couple of monolayers of overlaying metal play a significant role in the determination of the EWF of the whole system.[3] After the addition of two or three overlayers, the work function of the system becomes very similar to the bulk system of the overlying metal. In this letter, the minimum gate thickness necessary to fix the gate EWF is experimentally investigated. To do so, MOS capacitors with various TiN gate thicknesses were processed and controlled accurately. A boron doped polysilicon (poly-*p*+) is deposited on TiN as a cap in order to have a distinct work function of TiN and, thus, to evaluate influence of both work function (metal gate and cap stacked) on the EWF of the MOS capacitor. To control accurately the thickness of thin TiN layers, the pulsing chemical vapor deposition (CVD) technique, derived from the atomic layer deposition technique, was used. Indeed, films grown by this technique have attracted considerable attention due to the potential digital monitoring of film thickness by an appropriate number of reaction sequences (cycles).[4] During the growth, it is necessary to investigate the growth mode during the transient regime and the closure of the layer. Puurunen and Vandervost report that, in case of substrate-inhibited growth, the initial stage is constituted by an island growth regime growth leading to discontinuous layers.[5] The initial regime, the closure of the TiN layer, and its influence on the V_{FB} are presented in this letter.

In this work, thin films were deposited on thermally oxidized (100) silicon wafer. Prior to deposition, the SiO_2 substrates were cleaned by rapid thermal cleaning at 350 °C for 25 s. A pulsing CVD process has been developed using tetrakis-dimethylamido titanium and ammonia (NH_3).[6–8] During one cycle, precursors are sequentially introduced in the chamber and followed by a purge (N_2,He). The temperature of the substrate is kept at 180 °C and the pressure at 5 Torr. The initial stage of growth was studied using total x-ray fluorescence (TXRF). Atomic force microscopy (AFM) and scanning electron microscopy (SEM) were also employed to study the layer topography. Wavelength dispersive x-ray fluorescence (WDXRF) is used to estimate the average thickness of TiN layers. Fluorescence intensities were calibrated with x-ray reflectivity. The closure of the layer is studied by using static time of flight secondary ion mass spectrometry (TOFSIMS) with 25 keV Bi^+ incident ions. Simple MOS capacitors were fabricated by using a single damascene process on silicon *p*-type (100) oriented and boron implanted silicon substrate (doping level 2×10^{17} cm^{-3}). A conventional photolithography process was then used to define an active region of 0.0072 mm^2. Dry oxidation was then performed to grow the gate oxide (≈3 nm thick). Metallic TiN layers with various numbers of cycles were then deposited. A

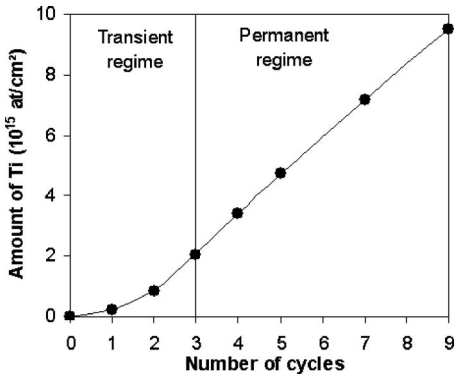

FIG. 1. Ti Amount (TXRF) deposited on the SiO_2 substrate as a function of the number of cycles.

a)Electronic mail: frederic.fillot@cea.fr.

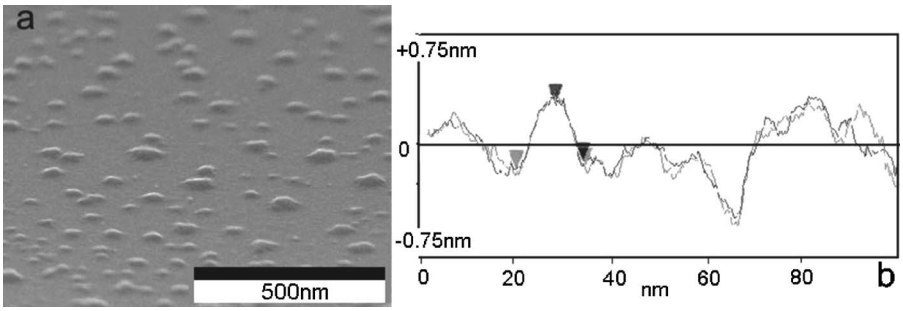

FIG. 2. (a) SEM image of one cycle of TiN deposited on thermal SiO_2. Prior observation, the sample was cleaned by a diluted HF solution, revealing the TiN islands. (b) AFM topography of one cycle of TiN deposited on thermal oxide.

boron doped Si-polycap (poly-*p*+) was then deposited at 580 °C on TiN to obtain electrical contact. All samples were annealed in N_2, H_2 gas at 425 °C for 30 min in order to reduce fixed oxide charges. The thermal budget is limited to 425 °C to prevent interdiffusion in the gate stack. High frequency capacitance-voltage (*C-V*) characteristics were measured at 100 kHz. The V_{FB} was compared with the full consistent quantum modelling of MOS capacitor *C-V* characteristics.[9]

Figure 1 shows the Ti amount deposited on silicon oxide as a function of the number of cycles. In agreement with Lim *et al.* observations, which also used SiO_2 substrates and similar reactants, two regimes can be distinguished: a transient and a permanent regime.[10–12] The permanent regime appears after three deposition cycles. A linear relationship is observed between the deposited Ti amount and the number of cycles. In this regime, the 7 Å/cycle growth rate is independent of the substrate (Figs. 1 and 3). This means that TiN grows on TiN. This high growth rate value, also observed by Kim *et al.* and Elam *et al.*, is explained by Sakuma *et al.* as a rechemisorption of reactants on the formed layer.[6,7,13] Below three cycles, a region with a very low growth rate is representative of the transient regime of growth. This lower growth characterized by the substrate-inihibited growth leads to islands formation of TiN and a discontinuous layer. Figure 2 shows a layer elaborated after one deposition cycle. The formation of islands of TiN on the substrate is clearly observed. For SEM observations [Fig. 2(a)], the sample was cleaned with diluted HF, which specifically etches the SiO_2 substrate, thus increasing the topography contrast for the SEM observation. AFM topography [Fig. 2(b)] shows also the presence of islands of TiN after one cycle. In both observations, the island size is similar and is smaller than 100 nm. For layers elaborated with various numbers of cycles, the AFM technique permits us to calculate the R_{max} which corresponds to the difference between the top point and the bottom point of the TiN layer on a surface of 2×2 μm^2. On each of these samples, the TiN effective thickness is estimated by measuring the Ti fluorescence intensity signal using WDXRF. In order to evaluate the closure of the layer, R_{max} was compared to the estimated TiN thickness. If the effective thickness is superior to the R_{max}, we conclude that the layer is continuous. Figure 3 shows the evolution of the effective thickness and R_{max} as a function of the number of cycles. As both curves intersect between three and four cycles of TiN deposition, we determine that a nearly 2 nm thick continuous layer is achieved for three or four cycles. The presence of the inflection point at three cycles on Fig. 1 and the intersecting point between R_{max} and the estimated thickness on Fig. 3 are in good agreement. These features indicate that a major change in the growth mode occurs in the vicinity of this point and is most likely to be a complete coverage of the silicon oxide surface with TiN. Finally, to check this observation, a static TOFSIMS experiment analyzing the chemical composition of the surface has been carried out to characterize the film closure. Figure 4 shows the integrated intensities of $^{28}Si^+$ and $^{48}Ti^+$ ions emitted from the surface as a function of the number of cycles. For zero and one cycle, $^{28}Si^+$ ions are observed while they vanish for three and four cycles. Similarly, $^{48}Ti^+$ ions are not emitted from the surface for zero cycle. $^{48}Ti^+$ ions are emitted for one cycle and reach a steady level for three and four cycles. These observations show that, for one cycle, the surface is constituted by SiO_2 and TiN, while starting at three cycles, the SiO_2 is fully covered by TiN. TOFSIMS measurements validate that a continuous TiN layer is formed from three cycles. To check the thickness of the TiN layer after three cycles of TiN process, high resolution transmission electron microscopy (HRTEM) observations have been made on the MOS capacitors. As shown in Fig. 5, the layer thickness of

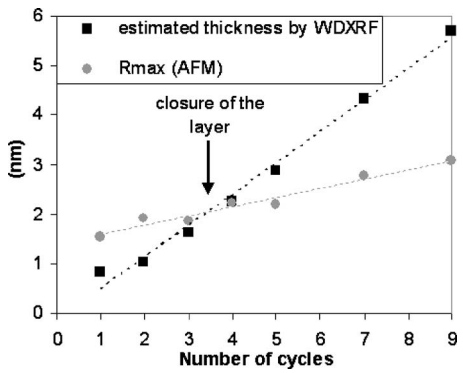

FIG. 3. Average TiN thickness estimated by WDXRF and R_{max} of TiN layer as a function of the number of cycles.

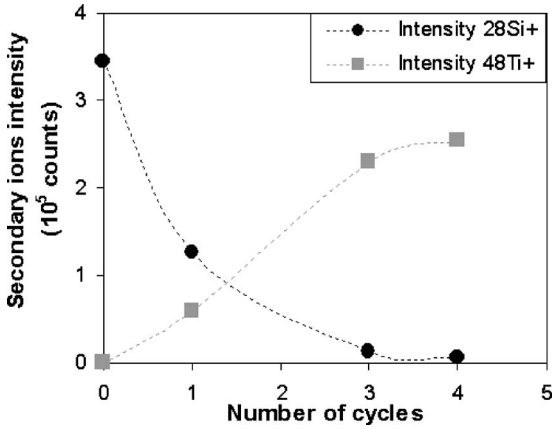

FIG. 4. Integrated area of the secondary intensity mass peaks ($^{28}Si^+$ and $^{48}Ti^+$) as a function of the number of cycles.

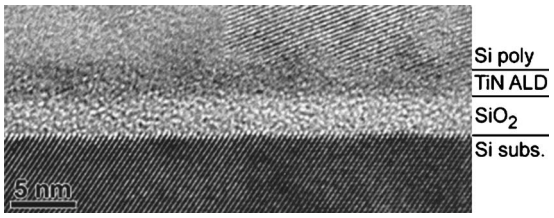

FIG. 5. Cross-section HRTEM image of $Si/SiO_2/TiN$ (three cycles)/poly-$p+$ capacitors.

TiN (≈2.3 nm) is equivalent to the value (≈2.2 nm) estimated by fluorescence. No significant evidence of interdiffusion between poly-$p+$ and TiN is observed from microscopy observations.

Capacitance-voltage (C-V) measurements are shown on Fig. 6. Changes in V_{FB} are observed. Generally, they can either be due to oxide charges or EWF changes. As the mechanical stress of TiN is low (−290 MPa) and as the thermal annealing are optimized, the contribution of oxide charges is not significant (<0.03 V) compared to the order of variation in the V_{FB} observed on the Fig. 5. Thus, during the initial stage of growth (< three cycles), the variation of V_{FB} as a function of the number of cycles is essentially due to changes in the EWF of the MOS capacitors. The C-V curves are overlayed for three and four cycles and after. As for zero and one cycle, gate is constituted or partially constituted of poly-Si, the maximum capacitance is lower compared to TiN gate (three and four cycles) due to polydepletion of poly-Si. Figure 7 shows the evolution of the V_{FB} as a function of the TiN effective thickness. The V_{FB} boron doped gate without TiN (zero cycle) was also measured (−0.26 V) to estimate the EWF of poly-$p+$. The value is lower than expected but we speculate that this low value is attributed to the inactivation of the boron doping species with low thermal anneal. During the initial growth of TiN (one cycle), an average V_{FB} between TiN and poly-$p+$ is measured (−0.54 V). As shown previously, the layer is, in this case, discontinuous and as the capacitor surface is large compared to the islands, both TiN and poly-$p+$ influence the EWF of the MOS capacitor and result in an average EWF between the both materials. After the closure (thickness >2.2 nm), the V_{FB} is independent of the TiN thickness (−0.73 V). Similar values of V_{FB} are obtained for a TiN thickness of between 2.2 and 7.1 nm. No variation has been also observed for thicker TiN films. We

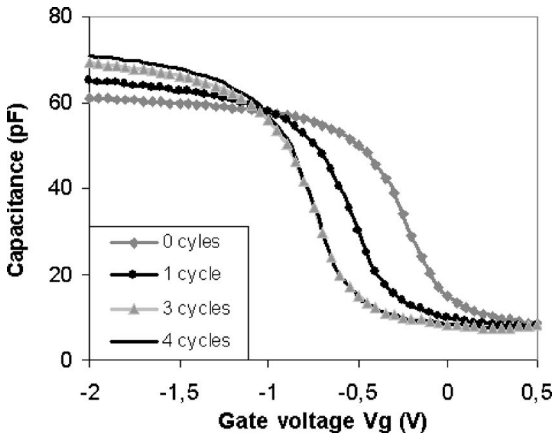

FIG. 6. Capacitance vs applied voltage at 100 kHz of MOS capacitors obtained with zero, one, three, and four cycles of TiN.

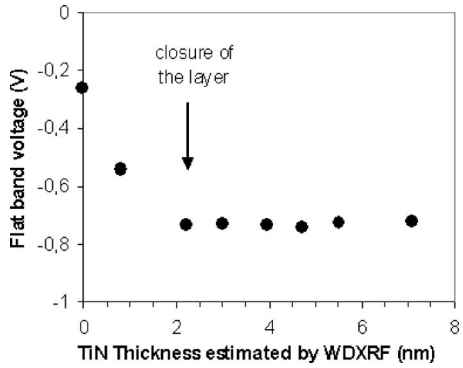

FIG. 7. Flatband voltage evolution of $Si/SiO_2/TiN/$poly-$p+$ capacitors as a function of the number of cycles.

conclude that the EWF of the MOS capacitors is independent of the TiN effective thickness. This indicate that the EWF is determined by the nature of the layer in contact with the dielectric (part of the layer <2.2 nm). The invariance of EWF may suggest that no penetration of the tail of the electron wave function of poly-$p+$ through the very thin TiN layer occurs.

In summary, we have studied the influence of the TiN thickness on the EWF of a MOS capacitor. We have found that a thin continuous TiN film of 2.2 nm is sufficient to determine the flatband voltage and the EWF of the MOS capacitor. We show experimentally that the EWF is only dependent on the properties of the interface (layer <2.2 nm) in contact with the gate dielectric. These results are in fairly good agreement with *ab initio* calculations by Park *et al.* which indicate that the couple of monolayers of overlaying metal play a significant role in the determination of the effective work function of the whole system.[3]

The authors gratefully acknowledge T. Morel, B. Guillaumot, and Y. Morand for stimulating discussions, and Y. Campidelli and V. Vidal for characterizations. This work was partially funded by the European "NanoCMOS" program, by the French Basic Technological Research (RTB) program and by Applied Materials.

[1]ITRS, International Technology Roadmap of Semiconductor 2006 update, http://public.itrs.net/
[2]C. Hobbs, L. Fonsesca, V. Dhandapani, B. Taylor, J. Grant, L. Dip, D. Triyoso, R. Hegde, D. Gilmer, R. Garcia, D. Roan, L. Lovejoy, R. Rai, L. Hebert, H. Tseng, B. White, and P. Tobin, Tech. Dig. VLSI Symp. **2003**, p. 9.
[3]S. Park, L. Columbo, Y. Nishi, and K. Cho, Appl. Phys. Lett. **86**, 073118 (2005).
[4]T. Suntola, *Handbook of Thin Film Process Technology* (Institute of Physics (IOP), Bristol, UK, 1996).
[5]R. L. Puurunen and W. Vandervost, J. Appl. Phys. **96**, 7686 (2004).
[6]H. K. Kim, J. Y. Kim, J. Y. Park, Y. Kim, Y. D. Kim, and H. Jeon, J. Korean Phys. Soc. **41**, 739 (2002).
[7]J. W. Elam, M. Schuisky, J. D. Ferguson, and S. M. George, Thin Solid Films **436**, 145 (2003).
[8]F. Fillot, T. Morel, S. Minoret, I. Matko, S. Maîtrejean, B. Guillaumot, B. Chenevier, and T. Billon, Microelectron. Eng. **82**, 248 (2005).
[9]R. Clerc, A. S. Spinelli, G. Ghibaudo, C. Leroux, and G. Pananakakis, Microelectron. Reliab. **41**, 1027 (2001).
[10]J. W. Lim, H. S. Park, and S. W. Kang, J. Electrochem. Soc. **148**, C403 (2001).
[11]J. W. Lim, H. S. Park, and S. W. Kang, J. Appl. Phys. **88**, 6327 (2000).
[12]J. W. Lim, J. S. Park, and S. W. Kang, J. Appl. Phys. **87**, 4632 (2000).
[13]Y. Sakuma, S. Muto, K. Nakajima, and N. Yokoyama, Appl. Surf. Sci. **82-83**, 239 (1994).